Send Orders of Reprints at bspsaif@emirates.net.ae

14 *Current Nanoscience,* 2013, *9,* 14-20

Investigation of Polymeric Composite Films Using Modified TiO_2 Nanoparticles for Organic Light Emitting Diodes

Do Ngoc Chung[1], Nguyen Nang Dinh[1]*, David Hui[2], Nguyen Dinh Duc[1], Tran Quang Trung[3] and Mircea Chipara[4]

[1]*University of Engineering and Technology, Vietnam National University, Hanoi, 144 Xuan Thuy Road, Cau-Giay District, Hanoi, Vietnam;* [2]*The University of New Orleans, Department of Mechanical Engineering, New Orleans, LA, USA;* [3]*University of Natural Science, Vietnam National University, Ho Chi Minh City, 227 Nguyen Van Cu Road, District 5, Ho Chi Minh City, Vietnam;* [4]*Mircea Chipara, The University of Texas Pan-American, Department of Physics and Geology, Edinburg, 78541, TX, USA*

Abstract: Nanocomposite films for hole transport and emitting layer were prepared from poly(3,4-ethylenedioxythiophene), poly(styrenesulfonate), and poly[2-methoxy-5-(2'-ethylhexyloxy)-1,4-phenylene vinylene] - as MEH-PPV - incorporated with anatase (TiO2) nanoparticles dispersed in oleic acid. The precursor for the sol was a solution of tetraiso-propyl orthotitanate [$Ti(iso\text{-}OC_3H_7)_4$]. The research showed that both the electrical and spectral properties of the conjugated polymers were enhanced due to the incorporation of anatase. The best volume ratio between the oleic acid precursor and tetraiso-propyl orthotitanate was found to be of 10. Current-voltage characteristics of organic light emitting diodes made from these nanocomposite films were considerably enhanced in comparison with those made from pure polymers. The luminous efficiency is reported. Mechanical properties of the nanocomposite materials, (in particular for MEH-PPV-TiO_2) were found to be dependent on constituent organic and inorganic materials and on the geometric position of constituents. It was concluded that such composite organic light emitting diodes can exhibit larger performance efficiency and longer lifetimes than classical light emitting diodes.

Keywords: Conducting polymers, current-voltage characteristics, energy gap, luminous efficiency, nanocomposite, organic light emitting diodes, photoluminescence, TiO_2 nanoparticles.

1. INTRODUCTION

Organic light emitting diodes (OLEDs) have been intensively investigated during the last decade, because of their potential applications (such as optoelectronics, urban lighting, screen for TV and cellular phones, large-area displays, solar flexible cells, etc [1-4]). However, in order to replace the light emitting diodes (LEDs) based on inorganic semiconducting materials it is necessary to improve both the efficiency and time of service of the OLEDs. While OLEDs and in particular polymer-based OLEDs did not yet reach the efficiency of inorganic LEDs, the difference between LEDs and OLEDs efficiencies is decreasing continuously. Polymeric LEDs are expected to present several advantages such as low cost (derived from the anticipation of future technologies, which will allow the printing of polymeric LEDs), outstanding mechanical properties (including flexibility), reduced weight, low operational voltage (by replacing ITO with conducting polymers), and good quantum efficiency. The lifetime of OLEDS is typically restricted by environmental issues (most important being represented by oxygen, water or moisture, and polymer aging) and intrinsic contributions controlled by atom diffusion and interfacial processes. Research efforts are aiming in particular at increasing the efficiency and the lifetime of polymer-based LEDs.

The mechanical properties of composite materials (and in particular of nanocomposites) are strongly dependent on the constituent materials nature, size, and concentration as well as on the interface between the polymeric matrix and the nanofiller, on the manufacturing technology, and on geometric position of constituents in the composite/final product. Up to now, many researchers have investigated mechanical properties of polymer composite reinforced by nanoparticles [5-8]. They tried to explain the mechanical properties of polymer-based nanocomposites by neglecting the interactions between nanoparticles. A brief analysis of the mechanical properties of OLEDs, which takes into account the interactions between nanoparticles, is presented.

The efficiency of the optoelectronic devices like OLED, is controlled by three factors: (i) equalization of injection rates of positive (hole) and negative (electron) charge carriers (ii) recombination of the charge carriers to form singlet exciton in the emitting layer (EML) and (iii) radiative decay of excitons. Recently, novel approaches to deal with these problems have been reported [9, 10] such as the addition of a hole transport layer (HTL) between the transparent anode and the emitting layer (EML) [9] and/or of an electron transport layer (ETL) sandwiched between the EML and cathode [10]. With these solutions one can enhance the electroluminescent efficiency of OLEDs. However, the long-lasting service is sometimes limited. The other way to enhance both the efficiency and the service duration of the device is to use nanocomposite films instead of pure polymers (served as HTL and EML). Embedded nanoparticles of oxides can substantially influence the mechanical, electrical and optical properties of the polymer. For instance, thin films of nanocrystalline anatase (nc-TiO_2) particles dispersed within poly[2-methoxy-5-(2'-ethylhexyloxy)-1,4-phenylene vinylene] (MEH-PPV) were studied as photoactive material [11]. By adding a hole transport layer (HTL) and an electron transport layer (ETL) to the three-layer device, the equalization of injection rates of hole and electron was improved and a higher electroluminescent efficiency of the OLED was obtained [12]. However, a large difference between the structure of the inorganic material (ITO) and the organic polyethylene (3,4-dioxythiophene) (PEDOT) usually causes a poor interface contact between them. Recently, the role of nanocomposites obtained by embedding TiO_2 nanoparticles in PEDOT or MEH-PPV on the I-V characteristics of OLEDs made from these composites, was reported [12]. Since the TiO_2 nanoparticles used to make the composites were taken from commercial sources, it was difficult to modify their surfaces in order to reach atomically con-

*Address correspondence to this author at the University of Engineering and Technology, Vietnam National University, Hanoi, 144 Xuan Thuy Road, Cau-Giay District, Hanoi, Vietnam; Tel:/Fax: + 84 4 3754 9429;
E-mail: dinhnn@vnu.edu.vn

1875-6786/13 $58.00+.00

tinuous TiO_2/polymer interfaces (or heterojunctions). This strongly blocked the charge transport through these interfaces.

In this work, the results of the research on the preparation and modification of TiO_2 nanoparticles used for the fabrication of OLEDs, are reported. Structural, electrical and spectroscopic properties of the dispersive particles and the nanocomposite films of PEDOT+nc-TiO_2 and MEH-PPV+nc-TiO_2 as well as current-voltage (I-V) characteristics of the devices made from the films were investigated. The mechanical properties of MEH-PPV+nc-TiO_2 vs. TiO_2 volume are also analyzed.

2. EXPERIMENTAL

Sol-gel method was used to prepare nanoparticles of TiO_2 with modified surface. The catalyst was trimethylamino-N-oxide dihydrate $[(CH_3)_3NO.2H_2O]$ with oleic acid as the derivative chemical agent. The precursor for the sol is a solution of tetraiso-propyl orthotitanate $[Ti(iso\text{-}OC_3H_7)_4]$. The precursor was mixed with oleic acid ($C_{17}H_{33}COOH$) in water and $(CH_3)_3NO.2H_2O$. This mixture was stirred at 80°C for up to 2 hours (when the homogeneous clear orange was obtained). To find out the optimum volume of oleic acid, various volume ratios of oleic acid per the precursor (r), ranging from 1.5 to 10 (see Table **1**), were chosen. The spectroscopic properties of the TiO_2 solutions were measured in quartz cells. TiO_2 powder was obtained by pouring the solution onto silicon substrates followed by annealing at 180°C, in air, for 3 hours. Annealing at such a low temperature makes difficult the growing process of TiO_2 particles, consequently the size of particles can be maintained at the same size of the dispersed TiO_2.

To deposit nanocomposite films, MEH-PPV was dissolved in xylene (8 mg of MEH-PPV in 10 ml of xylene). TiO_2 was then embedded in PEDOT-PSS (PEDOT+nc-TiO_2) with 15 wt % of TiO_2 and in MEH-PPV with 20 wt % of TiO_2 (MEH-PPV+nc-TiO_2). These concentrations were taken from the optimal values of the TiO_2 embedded within these polymers, which were obtained and reported elsewhere [13], where commercial TiO_2 nanoparticles with 5 nm in size were utilized. Using dispersed nc-TiO_2 particles one can expect to enhance the energy and charge transport through the TiO_2/polymer interfaces. Both the ultrasonic and magnetic stirring at temperature of 45 °C was used to achieve a homogenous distribution of TiO_2 within these polymers The PEDOT+nc-TiO_2 and MEH-PPV+nc-TiO_2 were deposited onto ITO/glass substrates by spin coating, then heated at 120 °C in a vacuum of 1.33 Pa for 1 hour to evaporate completely the solvent. The thickness of polymer layers was controlled both by the spinning rate and the viscosity of the solution. Details of the heterojunctions of these devices are shown in Fig. (**1**). Each ITO/glass substrate slide consists of four devices, which have dimensions of 2 mm × 2 mm or 4 mm^2 in area.

The heterojunctions of the as obtained OLEDs are shown in Fig. (**1**). The following abbreviations will be used:

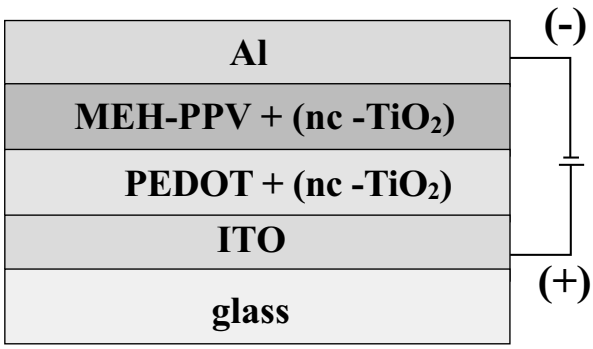

Fig. (1). Design of an OLED based on polymeric nanocomposites.

H1: PEDOT/MEH-PPV

H2: PEDOT/MEH-PPV+nc-TiO_2

H3: PEDOT+nc-TiO_2 /MEH-PPV

H4: PEDOT+nc-TiO_2/ MEH-PPV+nc-TiO_2

and for the devices made from corresponding heterojunctions:

NP0: ITO/PEDOT+nc-TiO_2/Al

N1: ITO/PEDOT/MEH-PPV/Al

N2: ITO/PEDOT/MEH-PPV+nc-TiO_2/Al

N3: ITO/PEDOT+nc-TiO_2 /MEH-PPV/Al

N4: ITO/PEDOT+nc-TiO_2/ MEH-PPV+nc-TiO_2/Al

The surface morphology of samples was characterized by using a "Hitachi" Field Emission Scanning Electron Microscopy (FE-SEM). Atomic force microscope (AFM) images were obtained using a NT-MDT Atomic Force Microscope operating in a tunnel current mode. Nanocrystalline structures were investigated by X-Ray Diffraction (XRD) with a Bruker D-Advance-8 diffractometer using filtered Cu Kα radiation (λ = 0.15406 nm). Photoluminescence spectra (PL) were carried-out by using a FL3-2 spectrophotometer and Current-voltage (I-V) characteristics were measured on an Auto-Lab Potentiostat PGS-30. The ultraviolet-visible absorption spectra were carried out on a Jasco UV-VIS-NIR V570.

3. RESULTS AND DISCUSSION

3.1. Properties of Dispersive TiO_2

Fig. (**2**) shows the absorption spectra of TiO_2 solutions vs. the volume ratio of oleic acid per precursors. From this figure one can see that solely MEH-PPV exhibits a peak in UV-VIS, in agreement with experimental data reported elsewhere [13]. The absorption edge of the samples is blue shifted with the increase of the r ratio (see the left panel of Fig. **1**). The absorption edges corresponding to *r* equal from 1.5 to 10 are located from 354 nm to 308 nm.

Table 1. Volumes of Compound Taking Part in the Synthesis of Dispersed TiO_2 Particles in Oleic Acid with Different Ratio (r)

r	Acid oleic (ml)	Precursor (ml)	H_2O (ml)	Catalyst (ml)
1.5	3.6	2.40	4.25	1.85
2.0	3.6	1.80	3.75	1.60
3.0	3.6	1.20	3.00	1.25
5.0	3.6	0.72	2.50	1.00
7.0	3.6	0.52	2.25	0.85
10.0	3.6	0.36	2.00	0.65

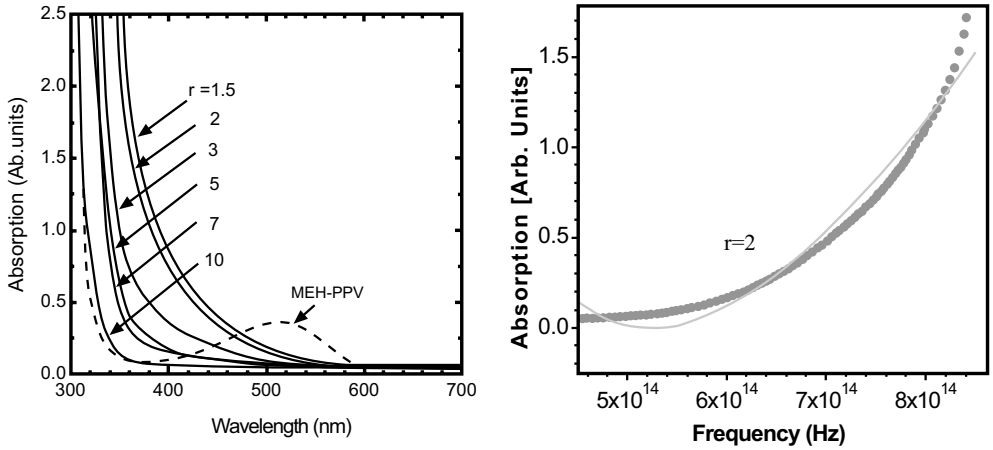

Fig. (2). Left panel: Absorption spectra of TiO_2-dispersed solutions with different concentration of oleic acid. Right Panel: Experimental data (gray line) and best fit (red line) for the sample with r=2 by using eq. 2.

Table 2. The Band Gap Value of Dispersed TiO_2 vs. r-ratio Estimated from the UV-Vis Spectra

Ratio (r)	1.5	2.0	3.0	5.0	7.0	10.0
E_G (eV)	2.15±0.05	2.17±0.05	2.16±0.05	2.24±0.05	2.33±0.06	2.37±0.07

UV-Vis data at short wavelength can be used to estimate the energy gap, E_G, of the dispersed nano-TiO_2 particles (Table **2**). by using the expression [14]:

$$\alpha = \frac{A}{h\nu}(h\nu - E_G)^n \quad (1)$$

Where h is Planck's constant, ν is the frequency of the incident UV-Vis radiation, A is a constant and n is 0.5 for direct band semiconductors and 2 for indirect band gap semiconductors. As expected, best fits were obtained for n=2 (indirect band).

The gap energies calculated from UV-VIS data were significantly smaller than the gap energy of pristine (bulk) TiO_2, which is in the range 3 to 3.3 eV [15]. This result is a contribution of several competing processes:

1. In confined semiconductors, the energy gap is size dependent [1], [13]:

$$E_G^{(R)} = E_G^{\infty} - \frac{1.8e^2}{\varepsilon R} + \frac{\hbar^2\pi^2}{8R^2}\left(\frac{1}{m_e} + \frac{1}{m_h}\right) \quad (2)$$

where $E_G^{(\infty)}$ is the energy gap of the bulk semiconductor, $E_G^{(R)}$ is the energy gap of a semiconductor of radius R, m_e is the effective mass of the electron, m_h is the effective mass of the hole, e represents the electronic charge, and ε the dielectric permittivity of the nanoparticle. The dependence of the energy gap on the particle size is rather complex due to the competition between the dipolar interaction term (second term in eq. 2), which tends to decrease the energy gap, and the confinement (last) term (which tends to increase the energy gap) [15]. In the case of TiO_2 nanoparticles such competition results in the increase of the energy gap as the size of nanoparticles is increased (for nanoparticles characterized by a diameter of 5 nm or larger) [15].

2. Nanocrystals have a high fraction of structural defects-due to their large surface to volume ratio. These defects can decrease the energy gap through the formation of defects' bands within the forbidden gap.

3. Actually, the gap energy was estimated for a composite that involve both conducting polymers and semiconducting nanoparticles. It is expected that the conducting polymer will decrease the energy gap of the semiconducting nanoparticles, typically via the opening of an impurity band within the energy gap of the semiconductor.

In order to identify the process responsible for the observed changes of the energy gap, complementary XRD investigations were performed. The XRD pattern of the TiO_2/Si sample made from the solution with the smallest r (i.e. r =1.5) shown in Fig. (**3**). There are six diffraction peaks which are quite consistent with the peaks for anatase phase of TiO_2 crystals [16]. Two intense peaks of the (021) and (211) directions correspond to the interplanar distances d = 0.240 nm and 0.192 nm, three weaker peaks of (111), (130) and (113) to 0.285 nm, 0.170 nm and 0.149 nm, respectively, and the weakest peak of (121) – to 0.212 nm. The fact that the peak width is rather large shows that the TiO_2 anatase powder consists of rather small particles. Scherrer formula was used to obtain the average particle size R:

$$R = \frac{0.9\lambda}{\beta\cos\theta} \quad (3)$$

where λ is wavelength of the X-ray used (λ = 0.15406 nm), β the peak width of half height in radians and θ the Bragg angle of the considered diffraction peak [17]. From the XRD patterns the average size of the particles was determined to range from 8 to 9 nm. The size of TiO_2/Si sample with the largest *r* was found to be of 7 nm (using the same procedure). Thus XRD results also confirmed the reduction of the particles size with the increase of the r-ratio (as the estimated size of TiO_2 nanoparticles is larger than 5 nm).

For the sample with r < 10, the absorption spectra edge of dispersed TiO_2 overlapped a part of the absorption spectra of MEH-PPV, for the sample with r ≥ 10, the absorption edge of TiO_2 did not affect to the absorption spectra of MEH-PPV (Fig. (**2**)). The volume ratio (r = 10) of oleic acid per the precursor [Ti(iso-$OC_3H_7)_4$] was used to synthesize and modify TiO_2 nanoparticles. The slight increase of the energy gap, reported in Table **2** is supported by the weak enhancement of the size of TiO_2 nanoparticles, as expected for TiO_2 clusters larger than 5 nm [15].

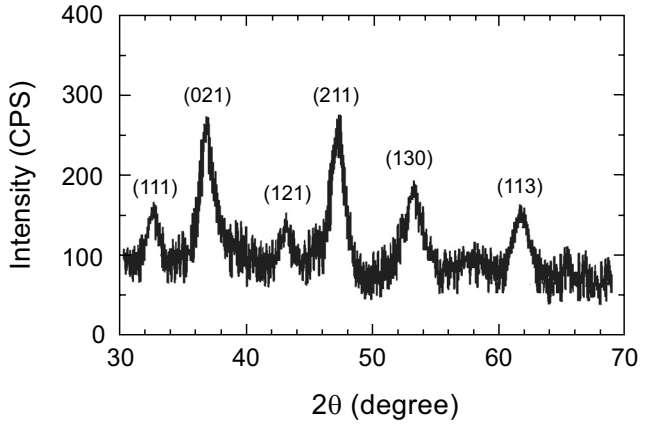

Fig. (3). XRD patterns of TiO_2 powders removed from silicon substrates for a TiO_2/Si sample with r = 1.5.

3.2. Nanocomposites Films

PEDOT has been used for the HTL in OLED because it has a high transmission in the visible region, a good thermal stability, and a high conductivity [18, 19]. To enhance the interface contact between ITO and PEDOT, dispersive TiO_2 nanoparticles were embedded within PEDOT. Fig. (**4**) shows the AFM of a PEDOT composite with a percentage of 15 wt % of dispersed TiO_2 nanoparticles (7 nm in size). With such a high resolution of the AFM one can see a distribution of nanoparticles in the polymer due to the spin-coating process. For the pure PEDOT, the surface exhibits smoothness comparable to the one of the area surrounding the nanoparticles. TiO_2 nanoparticles contributed to the roughness of the composite surface and created numerous TiO_2/ PEDOT boundaries in the composite film.

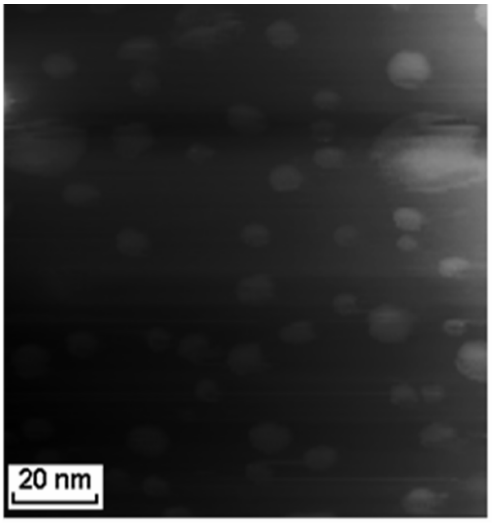

Fig. (4). AFM micrograph of a PEDOT+nc-TiO_2 nanocomposite film with 15 wt % of nc-TiO_2.

Surfaces of MEHPPV+TiO_2 nanocomposite films were examined by FE-SEM. Fig. (**5**) shows images of a nanocomposite sample with embedding of 20 wt % dispersed TiO_2 particles (7 nm in size). The surface of this film appears much smoother than the one of composites with a larger percentage of TiO_2 particles or with larger size TiO_2 particles. The influence of the heat treatment on the morphology of the films was weak, i.e. no noticeable differences in the surface were observed in samples annealed at 120°C, 150°C or 180°C in vacuum. The best annealing temperature for other properties such as the I-V characteristics and PL spectra was found to be 150 °C. In the sample considered, the distribution of TiO_2 nanoparticles is mostly uniform, except for a few bright points indicating the presence of nanoparticle clusters.

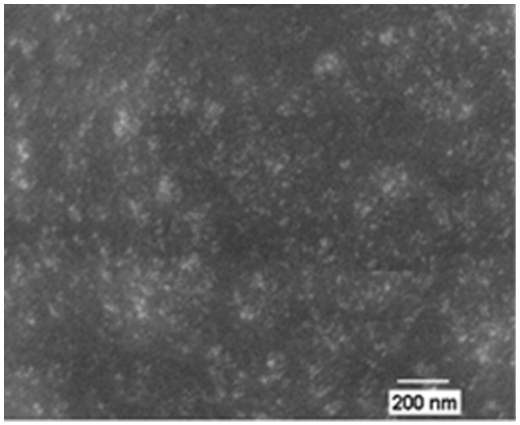

Fig. (5). FE-SEM micrograph of a MEH-PPV+nc-TiO_2 nanocomposite film (with 20 wt % nc- TiO_2 particles) used for the EL in OLED.

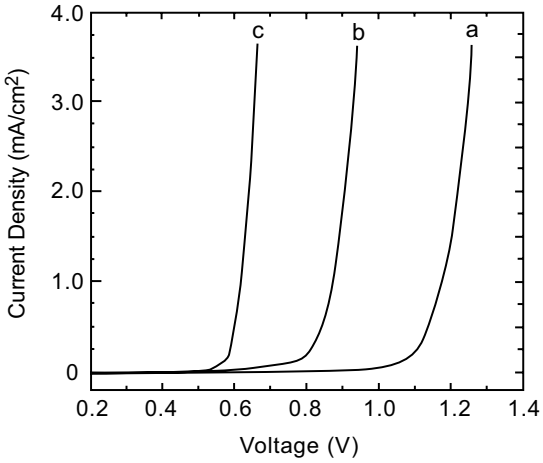

Fig. (6). I-V characteristics of the ITO/PEDOT+nc-TiO_2/Al device for a spin rate of 1500 rpm (a), 1700 rpm (b) and 2000 rpm (c).

Different spinning rate for coating were considered in order to find out optimal thickness of the thin composite films, The I-V characteristics vs. spinning rate of the heterojunction based on PEDOT+nc-TiO_2 (15 wt % of TiO_2) are shown in Fig. (**7**). From this figure one can see that the larger spin rate are associated with the smaller turn-on voltage of the device. At spinning rates larger or equal to 2000 rpm, the spun films were too thin and the I-V curve became worse. Thus, further spin rates of 2000 rpm were used to deposit PEDOT composite films. Similar results were observed for MEH-PPV+nc-TiO_2 (20 wt % of TiO_2) composite films, but a slight difference was obtained for the spin rate, i.e. the best spin rate was found to be of 2400 rpm. This can be explained by the different final thicknesses and TiO_2 concentrations of these polymers, as well as by the viscosities/solubilities of the conducting polymers.

In Fig. (**7**) the absorption spectra in the wavelength from 300 to 600 nm are presented. The inset shows the absorption spectra of the sample (in a shorter wavelength range, from 300 to 400 nm). It is seen that TiO_2 nanoparticles embedded in the films do not affect significantly the absorption spectra (as noticed in Fig. (**1**) for r = 10), except for a slight decrease of the absorption peak in composite

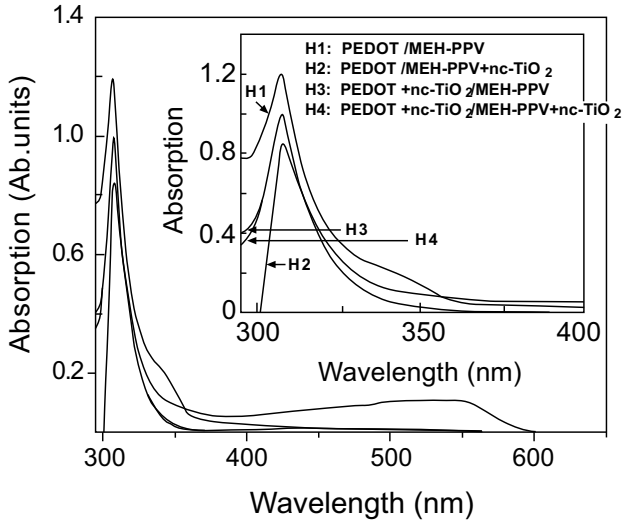

Fig. (7). Absorption spectra of OLEDs with use of different nanocomposites.

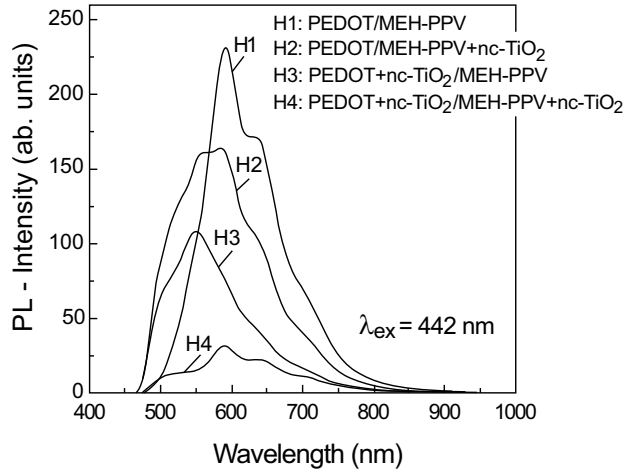

Fig. (8). Normalized photoluminescence spectra of PEDOT(+nc-TiO_2)/ MEH-PPV(+nc-TiO_2) thin films.

films. Perhaps, the presence of the TiO_2 particles dropped by a small quantity the amount of polymer within the nanocomposite, resulting in the reduction of their absorption. This is in good agreement with the results reported in [20] when the authors also used oleic acid for modifying TiO_2 that was embedded in MEH-PPV.

Photoluminescence spectra of the samples are shown in Fig. (**8**), demonstrating the so-called a quenching effect due to the addition of TiO_2 nanoparticles in the polymers. The mechanism of this reduction in PL spectra in MEH-PPV has already investigated [3, 20, 21]. The largest quenching was assigned to the presence of TiO_2 nanoparticles in both PEDOT and MEH-PPV. The blue shifts of PL spectra were also observed, in agreement with [21, 22] for ZnO nanoparticles. This blue shift is better observed for the H3 sample, which contains TiO_2 nanoparticles solely in PEDOT. As seen in Fig. (**8**), the sample H3 in comparison with H1 has a blue shift of the PL peak of about 40 nm. The blue shift can be explained by the change in band structure of PEDOT in the presence of TiO_2 nanoparticles [21-23].

Fig. (**9**) presents plots of I-V characteristics of the four devices (from N1 to N4) made from the heterojunctions (from H1 to H4). It

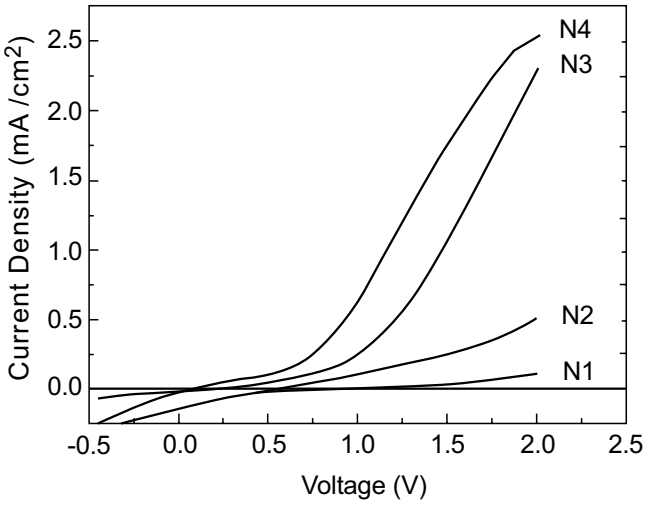

Fig. (9). I-V characteristics of OLEDs with use of different nanocomposites films.

is very clear that the turn-on voltage is enhanced from N1 to N4 samples. The N4 device made from two composites of both the HTL and EL layers (with embedding the modified TiO_2 nanoparticles of 7 nm in size) has the best I-V characteristic where the smallest turn-on voltage (~ 0.75 V) and the highest slope of current density versus voltage were observed. From this figure one can see that the addition of small TiO_2 particles into MEH-PPV and PEDOT polymers, the performance efficiency of the device is expected to be improved.

The luminous efficiency of the classical (N1) and composite-based (N4) devices was measured by a "Labsphere LCS-100" system with an accessory for OLED. The luminous efficiency vs. luminescence for both devices is shown in Fig. (**10**). From this figure one can see that at the same value of the luminance, the composite device possesses a much larger luminance efficiency than the classical device. The abrupt increase in the efficiency was obtained for luminance of the order of 13 cd/m^2. This relates to the most effective current range corresponding polarized potentials that were applied onto the transparent anode (ITO), where the current density in the I-V characteristic raised with an abrupt value. It is clear that by adding TiO_2 nanoparticles inpolymer EML and HTL layers, one can improve the energy efficiency of OLEDs.

The effect of both the HTL and ETL on the enhancement of the I-V characteristics was well demonstrated, associated with the equalization process of injection rates of holes and electrons. But the reason why the nanoparticles can improve the device performance is still open for discussion. For instance, this enhancement has been assigned [24] to the stimulated emission of optically-pumped MEH–PPV films (in the presence of TiO_2 nanoparticles), while other authors [25] indicated that no evidence of line narrowing or changes in the line shape was noticed at different voltages, concluding that the mechanism for improved performance was distinctly different from that found in optically-pumped TiO_2/MEH–PPV films. This suggests that the optical scattering phenomenon was not causing an enhancement in the device performance. Another possible explanation is that the nanoparticle surfaces increase the probability of electron-hole recombination; however, this would result in a change in the external quantum efficiency, rather than the current density as it was observed.

From the data of PL spectra for the MEH-PPV and PEDOT composites, one can see the luminescence quenching of the composites (see Fig. **8**), for the heterojunctions in particular. Similar phenomena obtained for nanohybrid layers were explained by TiO_2/polymer interfaces causing a difference in the band gap

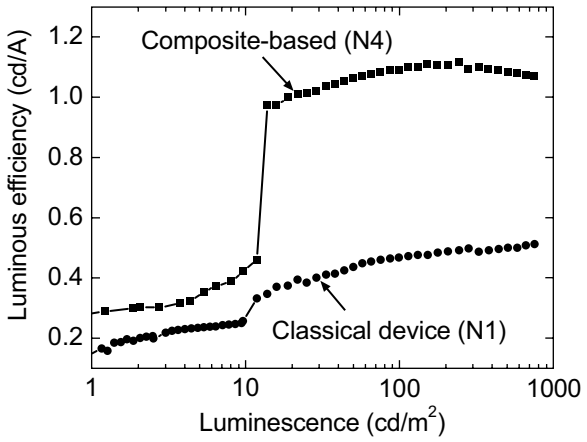

Fig. (10). The luminous efficiency of a composited based /N4 (top curve) and a classical device N1 (bottom curve).

between the oxide nanoparticles and the conjugate polymer [22-25]. Moreover, the results obtained for the improvement of I-V characteristics of PEDOT composite films (see Fig. **6**) prove that the spinning rate played an important role in the composite film polymerization. Based on these results, we would advance a hypothesis for the improved performance which supports the suggestion of Carter *et al.* [25]. A change in the device morphology would be caused by the incorporation of nanoparticles into the solution. During the spinning process in the spin-coating technique, the nanoparticles can adhere by strong electrostatic forces to the HTL and between themselves, and capillary forces can then draw the MEH–PPV solution around the nanoparticles into cavities without opening up pinholes through the device. This will result in a rough surface over which the aluminum cathode is evaporated and subsequently, a large surface area interface between the cathode and the electroluminescent composite material is formed. At a low voltage, charge-injection into MEH–PPV is expected to be cathode limited; the very steep rise in the I–V curves for the composite diodes suggests however that more efficient injection at the cathode through the heterojunctions is occurring. This could be correlated to a rougher interface of the nanocomposites. At a higher voltage, transport in MEH–PPV appears to be space-charge limited.

3.3. Mechanical Property of MEH-PPV+TiO_2 Composites (Theoretical Calculation)

In order to establish a model for resolving the problem how the nanoparticles which are embedded in polymer affects the mechanical properties and the lifetime of an OLEDs it was considered that all the nanoparticles are spherical with the same radius size of a (nm). The matrix and nanoparticles were assumed elastic, homogeneous, and isotropic being characterized by two independent and different elastic parameters, such as Young's (E) and bulk (K) modules.

When nanoparticles have infinitesimal sizes, nanocomposite materials will have nano effects, that is, interaction between constituents will appear and stress distribution in material will be represented as follows:

$$\sigma_{ik} = \sigma_{ik}^{0} + \sigma_{ik}^{*} + \sigma_{ik}^{**} + \ldots \quad (4)$$

where σ_{ik}^{0} to be homogeneous stress, σ_{ik}^{*} is interaction stress between matrix and particles, σ_{ik}^{**} interaction stress between the nearest particles, etc. For simplicity only the first and the second terms of Eq. (4) will be considered.

Assuming constituent materials to be homogeneous and isotropic, equilibrium equation in terms of displacement components is written as follows, known as Lame's equations:

$$2(1-\nu)\text{graddiv}\bar{u} - (1-2\nu)\text{rotrot}\bar{u} = 0 \quad (5)$$

Mechanical features can be described by resolving the equation (5) under the assumption that micro- and nano-stress of a spherical system is located at center of particles. The detail of the calculation was reported elsewhere [26]. Finally, one obtain, two new elastic properties for the composite material with nano spherical particles, as follows;

$$E_{eff} = \frac{9K_{eff}G_{eff}}{3K_{eff}+G_{eff}}, \quad \nu_{eff} = \frac{3K_{eff}-2G_{eff}}{6K_{eff}-2G_{eff}} \quad (6)$$

where;

$$K_{eff} = K\frac{1+4\xi_c GL(3K)^{-1}}{1-4\xi_c GL(3K)^{-1}}, G_{eff} = G\frac{1-\xi_c(7-5\nu)H}{1+\xi_c(8-10\nu)H} \quad (7)$$

$$L = \frac{K_c - K}{K_c - 4G/3}, \quad H = \frac{G/G_c - 1}{8-10\nu+(7-5\nu)G/G_c} \quad (8)$$

and ξ_c is volume fraction of nanoparticles, for instance in present work it is ranging from 0.10 to 0.20 corresponding to 0.15 ÷ 30 wt.%.

These formula can be applied, as a numerical example, for MEH-PPV+TiO_2 nanocomposites. From the data of polymers, MEH-PPV is characterized by $E = 70GPa$ and $\nu = 0.3$; TiO_2 has $E_c = 282.76GPa$ and $\nu_c = 0.28$ [27]. The calculation results obtained by equations (6) and (7) are plotted in Fig. (**11**).

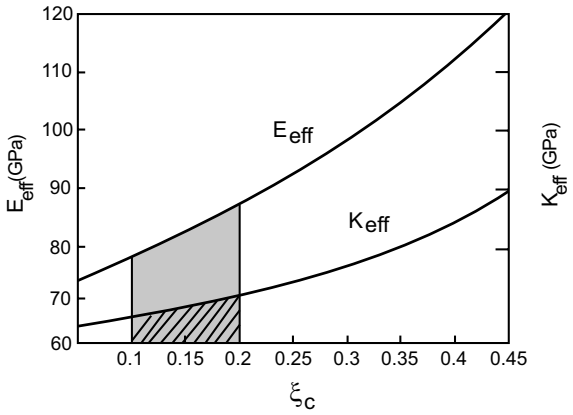

Fig. (11). Variation of effective Young's modulus (E_{eff}) and effective bulk modulus (K_{eff}) vs. the volume fraction ξ_c.

The marked areas in Fig. (**11**) show the range of the TiO_2 content embedded in polymers. From this one can notice that the dispersion of nc-TiO_2 nanoparticle within polymers have increased both the effective Young's (E_{eff}) and effective bulk modulus (K_{eff}). Consequently, the nanoparticles enhance the stability and lifetime of the component layers of the devices. Accordingly, a long-lasting service of the devices made from such nanocomposites is expected.

4. CONCLUSIONS

Nanocomposite films for a HTL and EML were prepared from PEDOT and MEH-PPV respectively, incorporated with TiO_2 nanoparticles dispersed in oleic acid. It was speculated that under certain circumstances the electric conduction in MEH-PPV (and in particular in MEH-PPV/conducting polymers) may be controlled by tunneling rather than image charges effects. The reduction of the

barrier height at the interface MEH-PPV:conducting polymers has been recently reported. These explain the existing enthusiasm in the study of MEH based polymeric OLEDs [28]. The study of the electrical and photoluminescent properties of the composites as well as of I-V characteristics of the OLEDs based on the composites showed that electrical, spectroscopic, and mechanical properties of the conjugate polymers were enhanced due to the incorporation of nc-TiO_2 within the polymers, especially when using the TiO_2 nanoparticles that were dispersed and modified in oleic acid with an appropriate volume ratio. The luminous efficiency of classical and composite based OLED devices was reported and the benefits of the nanocomposite approach to OLED devices was demonstrated. Mechanical properties of the nanocomposite materials, for MEH-PPV+nc-TiO_2 in particular were found to be dependent on both the constituent organic and inorganic components, as well as the geometric position of constituents. The improvement of the mechanical properties of the OLEDs through the dispersion of nanoparticles is predicted. The OLEDs made from the nanocomposite films would exhibit a larger photonic efficiency and a longer lasting life. Further improvements are expected by exploiting the self-assembly capabilities of polymeric thin films [29-32] through the use of block copolymers as polymeric component [31].

CONFLICT OF INTERESTS

All authors confirm the absence of any conflict of interests.

ACKNOWLEDGEMENTS

This work was supported by the MOST of Vietnam through the Project on Fundamental Scientific Research and Applications in 2011, Code: 1/2010/HD-DTNCCBUD. The research done by the University of New Orleans and The University of Texas Pan American was supported by DARPA under grant HR0011-08-1-0084 to AMRI - University of New Orleans.

ABBREVIATIONS

H1	=	PEDOT/MEH-PPV
H2	=	PEDOT/MEH-PPV+nc-TiO_2
H3	=	PEDOT+nc-TiO_2 /MEH-PPV/Al
H4	=	PEDOT+nc-TiO_2/ MEH-PPV+nc-TiO_2
NP0	=	ITO/PEDOT+nc-TiO_2/Al
N1	=	ITO/PEDOT/MEH-PPV/Al
N2	=	ITO/PEDOT/MEH-PPV+nc-TiO_2
N3	=	ITO/PEDOT+nc-TiO_2 /MEH-PPV/Al
N4	=	ITO/PEDOT+nc-TiO_2/ MEH-PPV+nc-TiO_2/Al

REFERENCES

[1] Salafsky, J. S. Exciton dissociation, charge transport, and recombination in ultrathin, conjugated polymer-TiO_2 nanocrystal intermixed composites. *Phys. Rev. B*, **1999**, *59*, 10885-10894.

[2] Burlakov, V. M.; Kawata, K.; Assender, H. E.; Briggs, G. A. D.; Ruseckas, A.; Samuel, I. D. W. Discrete hopping model of exciton transport in disordered media. *Phys. Rev. B*, **2005**, *72*, 075206-1-075206-5.

[3] Petrella, A.; Tamborra, M.; Cozzoli, P. D.; Curri, M. L.; Striccoli, M.; Cosma, P.; Farinola, G.M.; Babudri, F.; Naso, F.; Agostiano, A. TiO_2 nanocrystals – MEH-PPV composite thin films as photoactive material. *Thin Solid Films*, **2004**, *451/452*, 64-68.

[4] Spanggaard, H.; Kerbs, F. C. A brief history of the development of organic and polymeric photovoltaics, *Sol. Energy. Mat. Sol. Cells*, **2004**, *83*, 125-146.

[5] Suyev, Yu. S. Reinforcement of polymers by finely dispersed fillers (Review). *Polym. Sci. (USSR)*, **1979**, *21*, 1315-1336.

[6] Thomas, P. S.; Kuruvilla, J.; Sabu, T. Mechanical properties of titanium dioxide-filled polystyrene microcomposites. *Mater. Lett.*, **2004**, *58*, 281-289.

[7] Móczó, J.; Pukánszky, B. Polymer micro and nanocomposites: Structure, interactions, properties. *J. Industr.. & Eng. Chem.*, **2008**, *14*, 535-563.

[8] Choulis, S. A.; Mathai, M. K.; Choong, V.- E. Influence of metallic nanoparticles on the performance of organic electrophosphorescence devices. *Appl. Phys. Lett*., **2006**, *88*, 213503-213505.

[9] Markov, D. E.; Blom, P. W. M. Migration-assisted energy transfer at conjugated polymer/metal interfaces. *Phys. Rev. B,* **2005**, *72*, 161401(R)-161404(R)

[10] Kawata, K.; Burlakov, V. M.; Carey, M. J.; Assender, H. E.; Briggs, G. A. D.; Ruseckas, A.; Samuel I. D. W. Description of exciton transport in a TiO_2/MEH, PPV heterojunction photovoltaic material. *Sol. Energy Mat. Sol. Cells,* **2005**, *87*, 715-724.

[11] Ruhstaller, B.; Carter, S. A.; Barth, S.; Riel, H.; Riess, W.; Scott, J. C. Transient and steady-state behavior of space charges in multilayer organic light-emitting diodes. *J. Appl. Phys.*, **2001**, *89*, 4575-4586.

[12] Dinh, N. N.; Chi, L. H.; Chung Thuy, T. T.; Trung, T. Q.; Vo-Van, T. Enhancement of current, voltage characteristics of multilayer organic light emitting diodes by using nanostructured composite films. *J. Appl. Phys.,* **2009**, *105*, 093518-1-093518-6.

[13] Chung Thuy, T. T. *Preparation of nanostructured composites for Organic Light Emitting Diodes and, characterization of their electrical and spectro-optic properties*, Ph.D. Thesis (in Vietnamese). Hanoi, **2010**.

[14] Chipara, M.; Chipara, M. D. Uv-Vis investigations on ion beam irradiated polycarbonate. *E-Polymers*, **2008**, Article Number: *145*.

[15] Lin, H.; Huang, C. P.; Li, W.; Ni, C.; Shah, S. I.; Tseng, H-H. Size dependency of nanocrystalline TiO_2 on its optical property and photocatalytic reactivity exemplified by 2-chlorophenol. *Appl. Catal. B: Environm.*, **2006**, *68*, 1-11.

[16] ASTM files for crystalline structures; PDF No. 01-072-0021, ICSD No. 15328.

[17] Cullity, B. D. *Elements of X-Ray Diffraction*, 2nd ed., Addison-Wesley Publishing Company, Inc., Reading, MA, **1978** , p. 102.

[18] Quyang, J.; Xu, Q.; Chu, C.-W.; Yang, Y.; Li, G.; Shinar, J. On the mechanism of conductivity enhancement in poly(3,4, ethylenedioxythiophene):poly (styrene sufonate) film through solvent treatment. *Polymer*, **2004**, *45*, 8443-8450.

[19] Tehrani, P.; Kanciurzewska, A.; Crispin, X.; Robinson, N. D.; Fahlman, M.; Berggren, M. The effect of pH on the electrochemical over, oxidation in PEDOT:PSS films. *Solid State Ionics*, **2007**, *177*, 3521-3529.

[20] Lin, Y. -T.; Zeng, T. -W.; Lai, W. -Z.; Chen, C. -W.; Lin, Y. -Y.; Chang Y. -S.; Su, W. -F. Efficient photoinduced charge transfer in TiO_2 nanorod/conjugated polymer hybrid materials. *Nanotechnology*, **2006**, *17*, 5781-5785.

[21] Ton-That, C.; Phillips, R. M.; Nguyen, T. -P. Blue shift in the luminescence spectra of MEH-PPV films containing ZnO nanoparticles. *J. Lumines.*, **2008**, *128*, 2031-2034.

[22] Yang, S. H.; Nguyen, T. P.; Le Rendu, P.; Hsu, C. S. Optical and electrical properties of PPV/SiO_2 and PPV/TiO_2 composite materials. *Composites Part A: Appl. Sci. Manufact.*, **2005**, *36*, 509-513.

[23] Scott, J. C.; Kaufman, J.; Brock, P. J.; DiPietro, R.; Salem, J.; Goitia, J. A. MEH-PPV Light, Emitting Diodes: Mechanisms of Failure. *J. Appl. Phys.*, **1996**, *79*, 2745-2753.

[24] Chung Thuy, T. T.; Chi, L. H.; Dinh, N. N. Study of Photoluminescent and Electrical Properties of Nanostructured MEH, PPV/ TiO_2 hybrid films. *JKPS*, **2009**, *54*, 291-295.

[25] Carter, S. A.; Scott, J. C.; Brock, P. J. Enhanced luminance in polymer composite light emitting diodes. *Appl. Phys. Lett*., **1997**, *71*, 1145-1147.

[26] Vanin, G. A.; Duc, N. D. The theory of spherofibrous composite. 1: The input relations, hypothesis and models. *J. Mech. Compos. Mater.*, **1966**, *32*, 291-296.

[27] Selvin, J. A. P.; Kuruvilla, J.; Sabu, T. Mechanical properties of titanium dioxide-filled polystyrene microcomposites. *Mater. Lett.*, **2004**, *58*, 281-285.

[28] Yang, Y.; Heeger, A. J. Polyaniline as a transparent electrode for polymer light-emitting diodes: Lower operating voltage and higher efficiency. *Appl. Phys. Lett*., **1994**, *64*, 1245-1248.

[29] Zhou, Yong; Wang, Lian Z.; Ma, Ren Z.; Ebina, Yasuo; Takada, Kazunori; Sasaki, Takayoshi. Fabrication and Electrochemical Characterization of Molecularly Alternating Self-Assembled Films and Capsules of Titania Nanosheets and Gold Nanoparticles. *Curr. Nanosci.*, **2007**, *3*, 155-160.

[30] Shin, H.; Yukimichi, N. Polymer/Metal Nanocomposites: Assembly of Metal Nanoparticles in Polymer Films and their Applications. *Curr. Nanosci.*, **2007**, *3*, 206-214.

[31] Chipara, M.; Hui, D.; Sankar, J.; Leslie-Pelecky, D.; Bender, A.; Yue, L.; Skomski, R.; Sellmyer, D. J. On styrene–butadiene–styrene–barium ferrite nanocomposites. *Composites B*, **2004**, *35*, 235-243.

[32] Yu, S.-H.; Chen, S.-F. Recent Advances in Polymer Directed Crystal Growth and Mediated Self- Assembly of Nanoparticles. *Curr. Nanosci.*, **2006**, *2*, 81-92.

Received: June 18, 2012 **Revised: September 4, 2012** **Accepted: September 28, 2012**